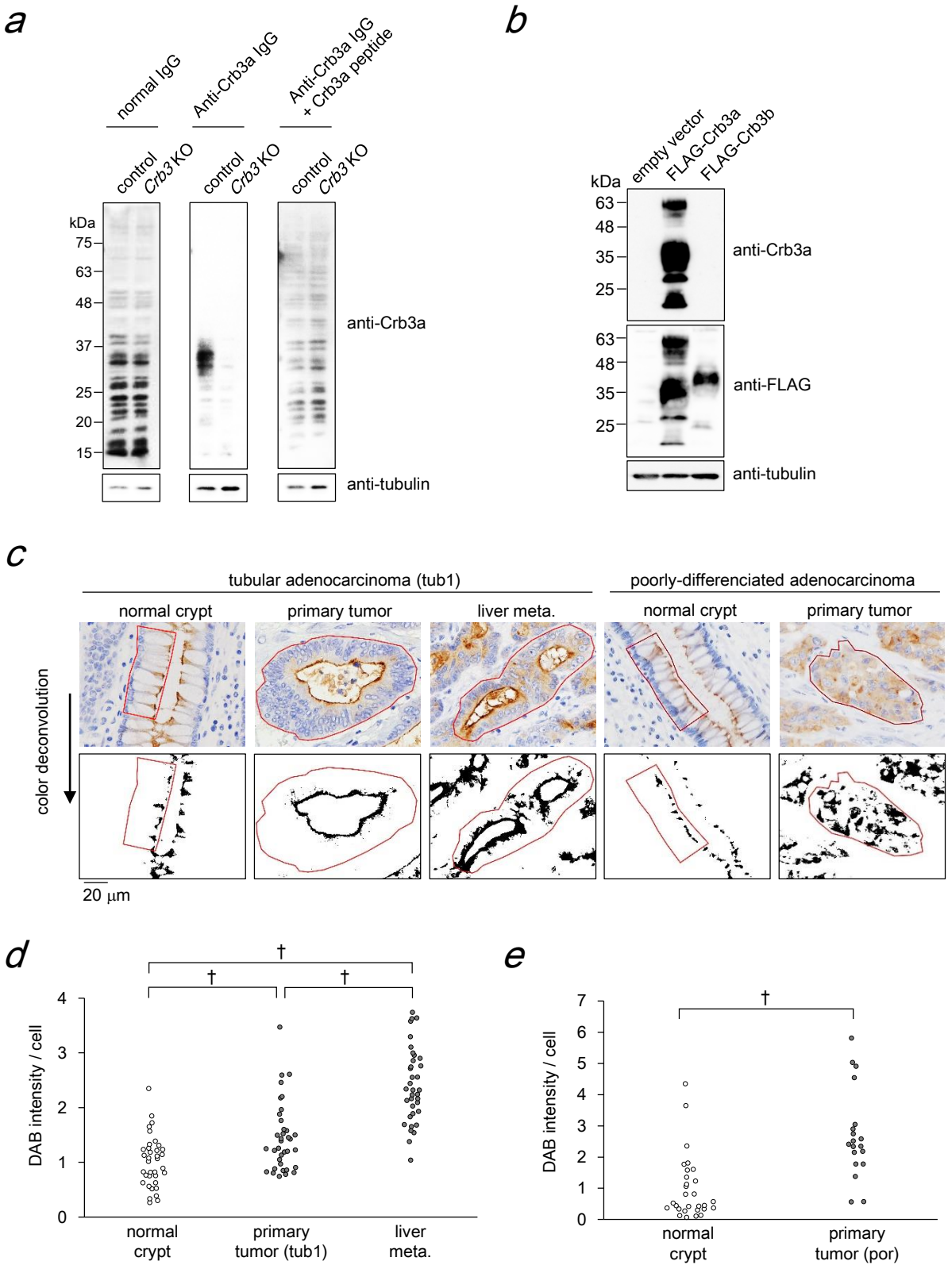

Supporting Information Figure 1 Iioka et al.

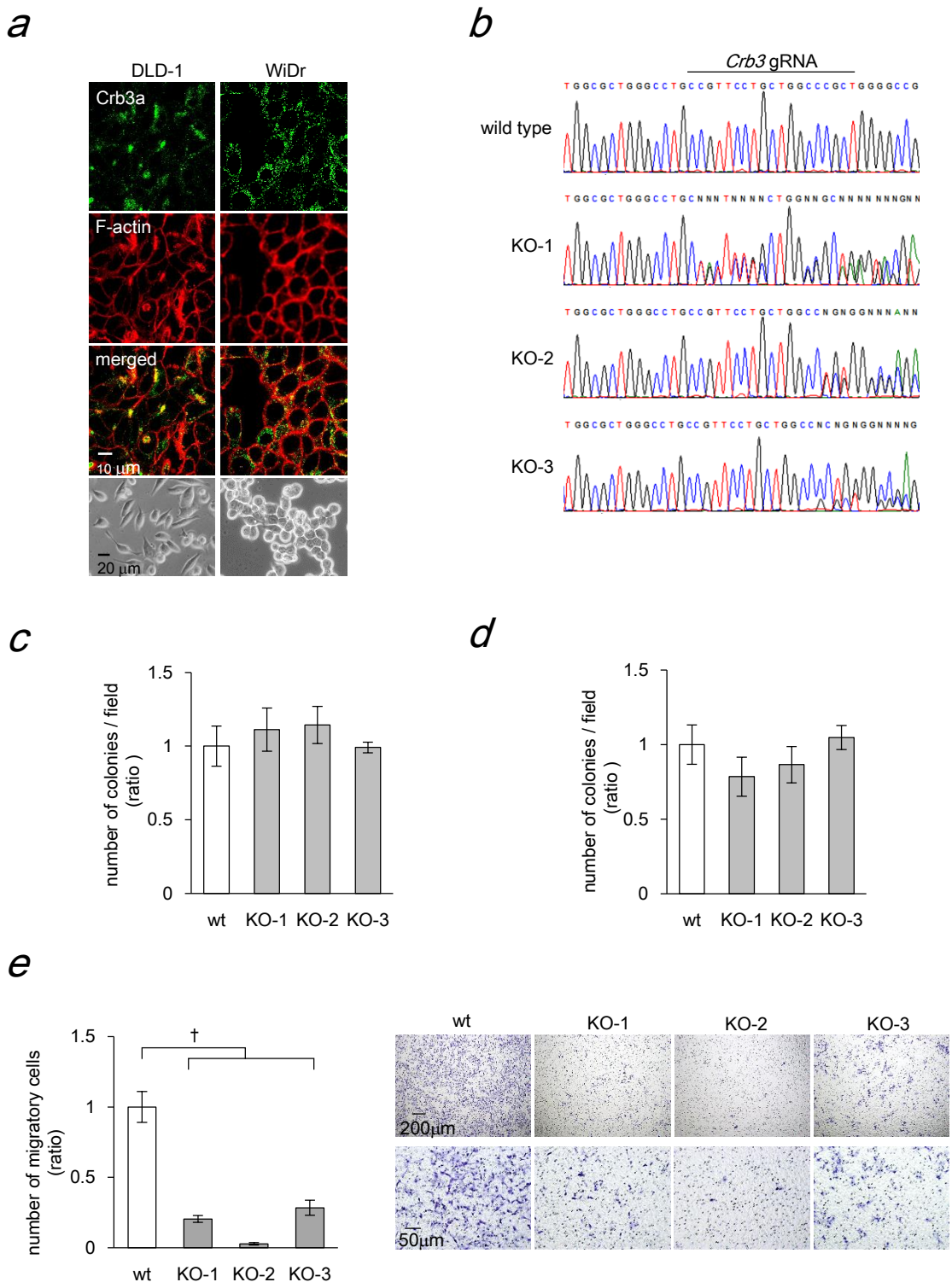

Supporting Information Figure 2 Iioka et al.

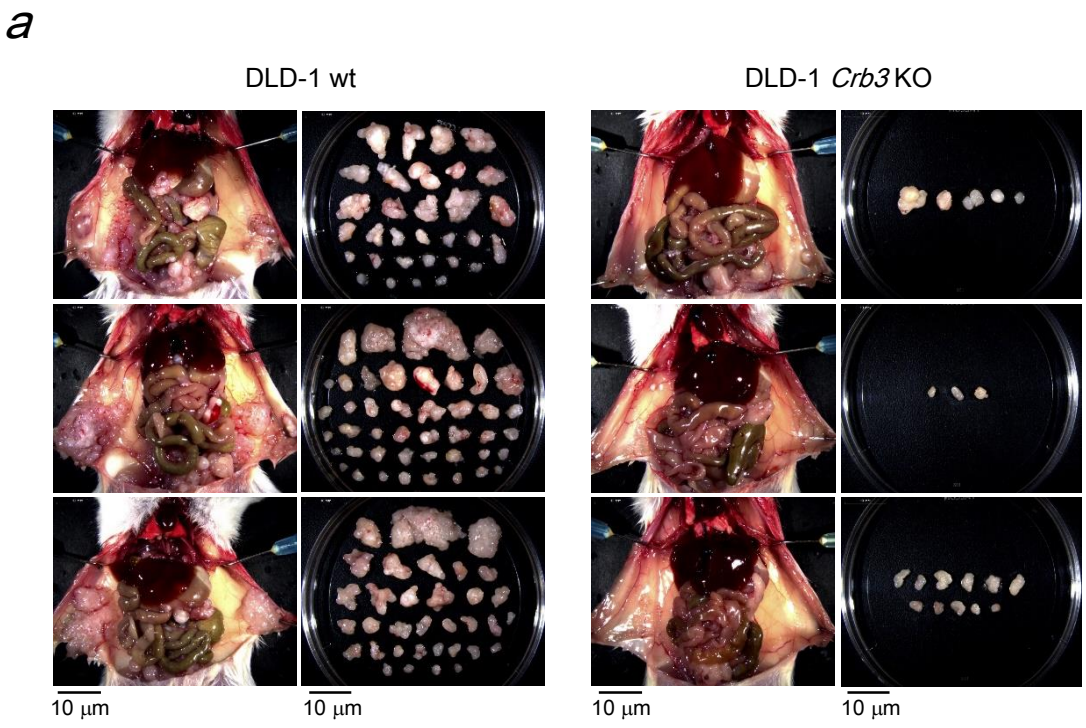

Supporting Information Figure 3 Iioka et al.

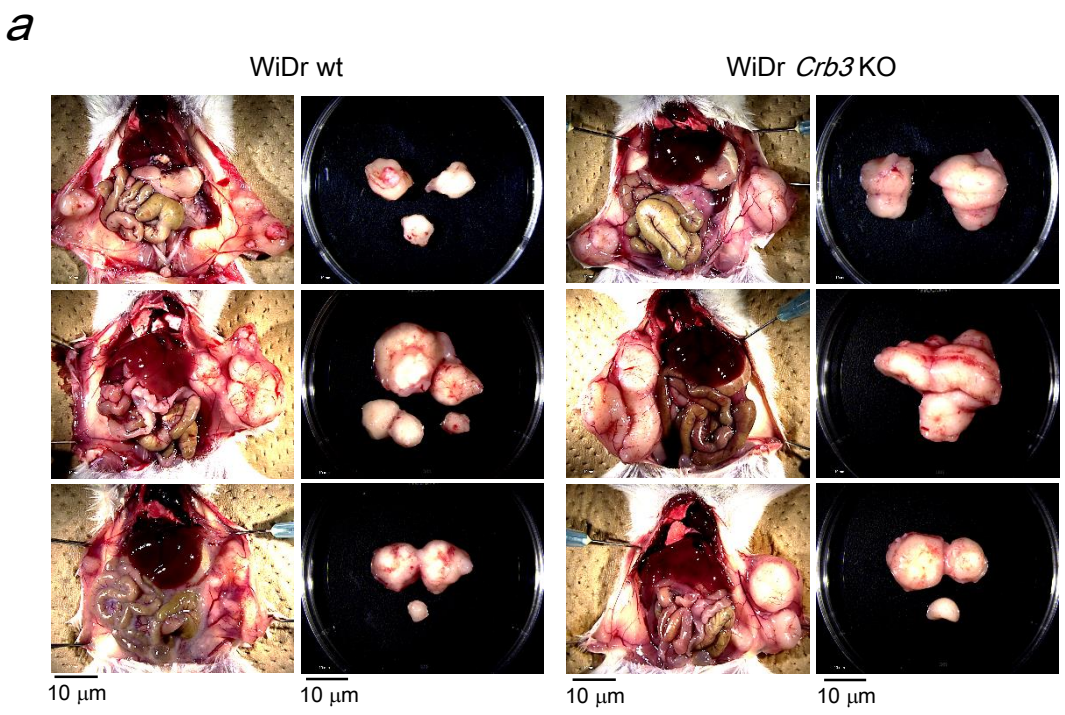

Supporting Information Figure 4 Iioka et al.

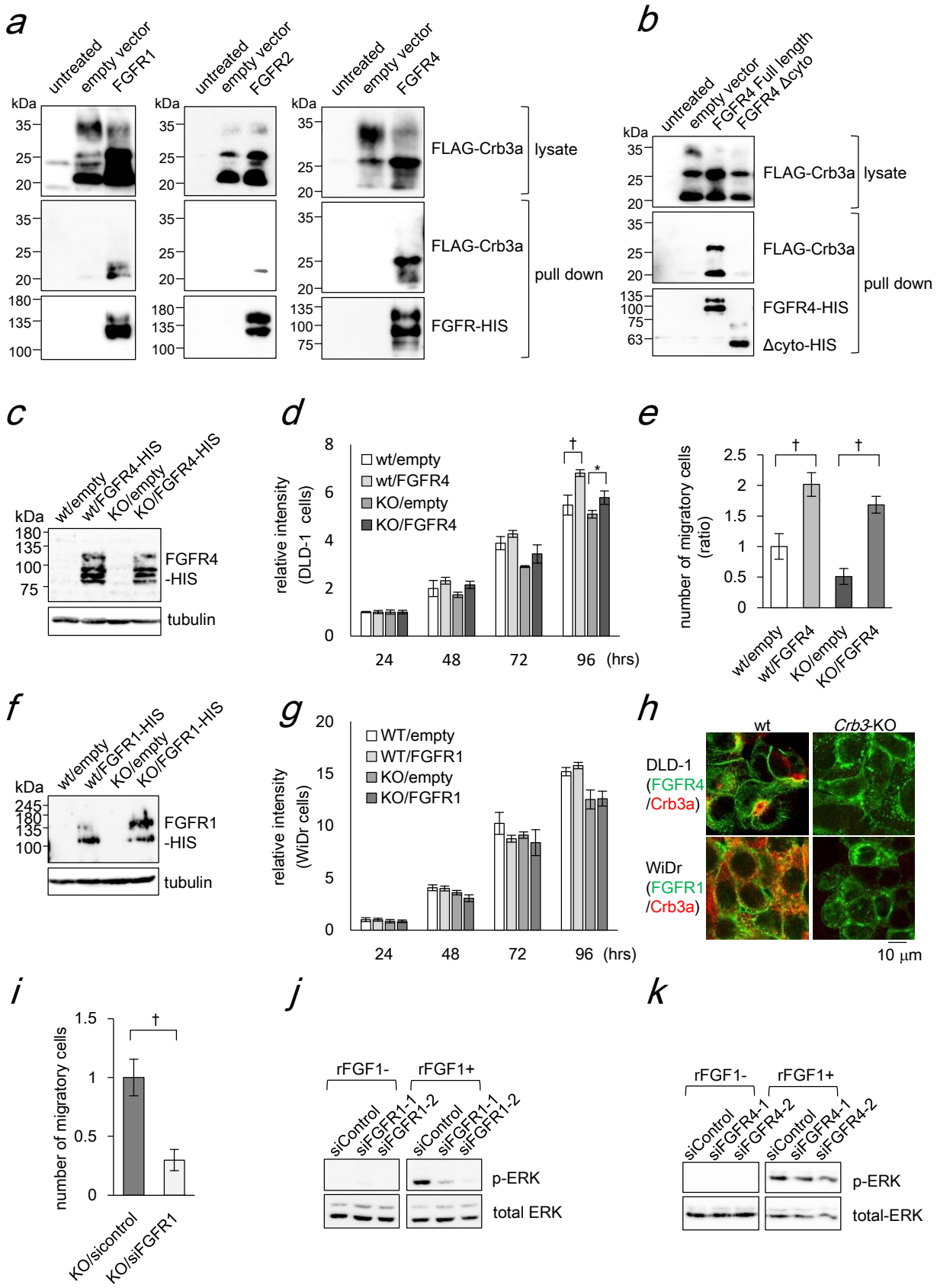

Supporting Information Figure 5 Iioka et al.

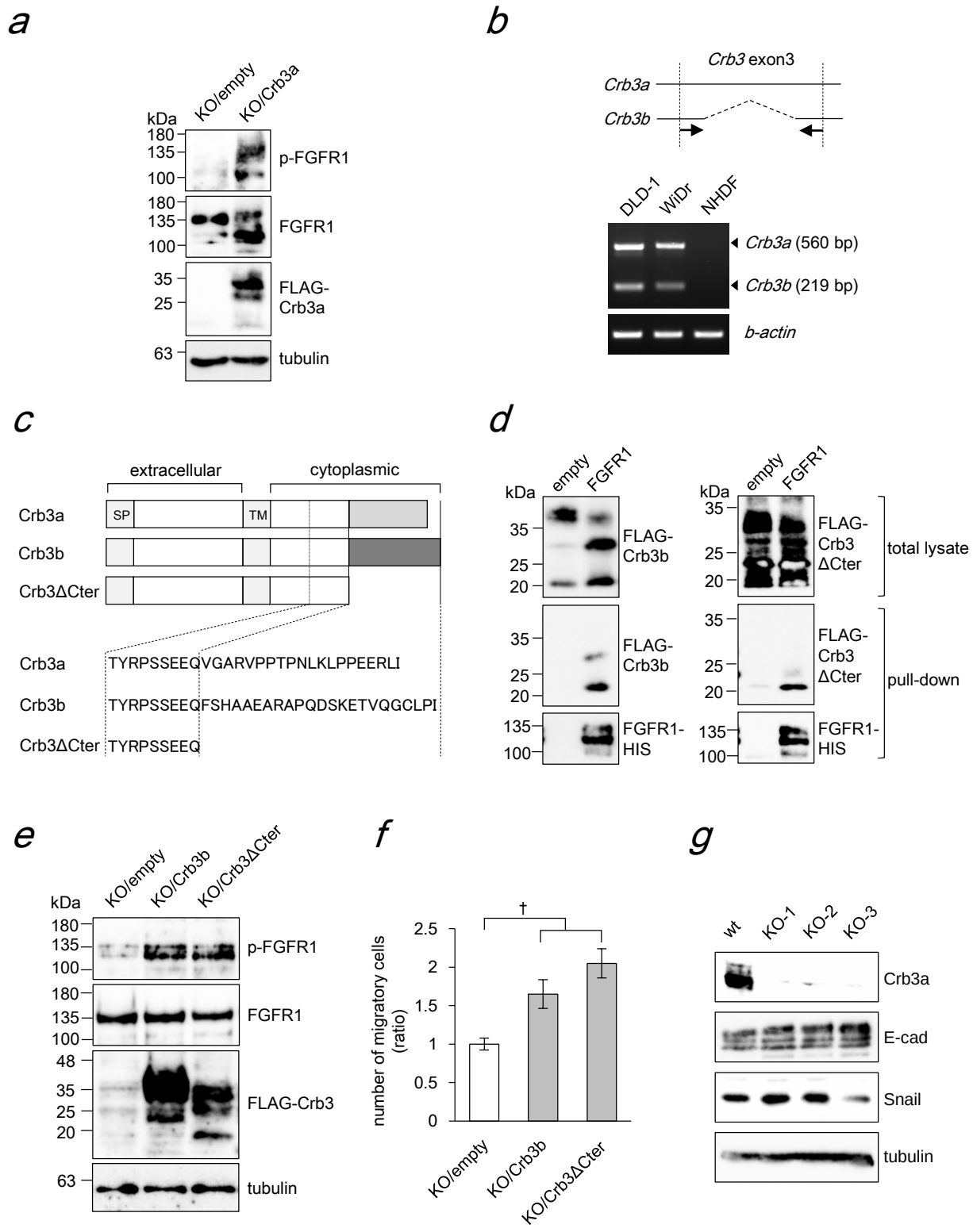

Supporting Information Figure 6 Iioka et al.

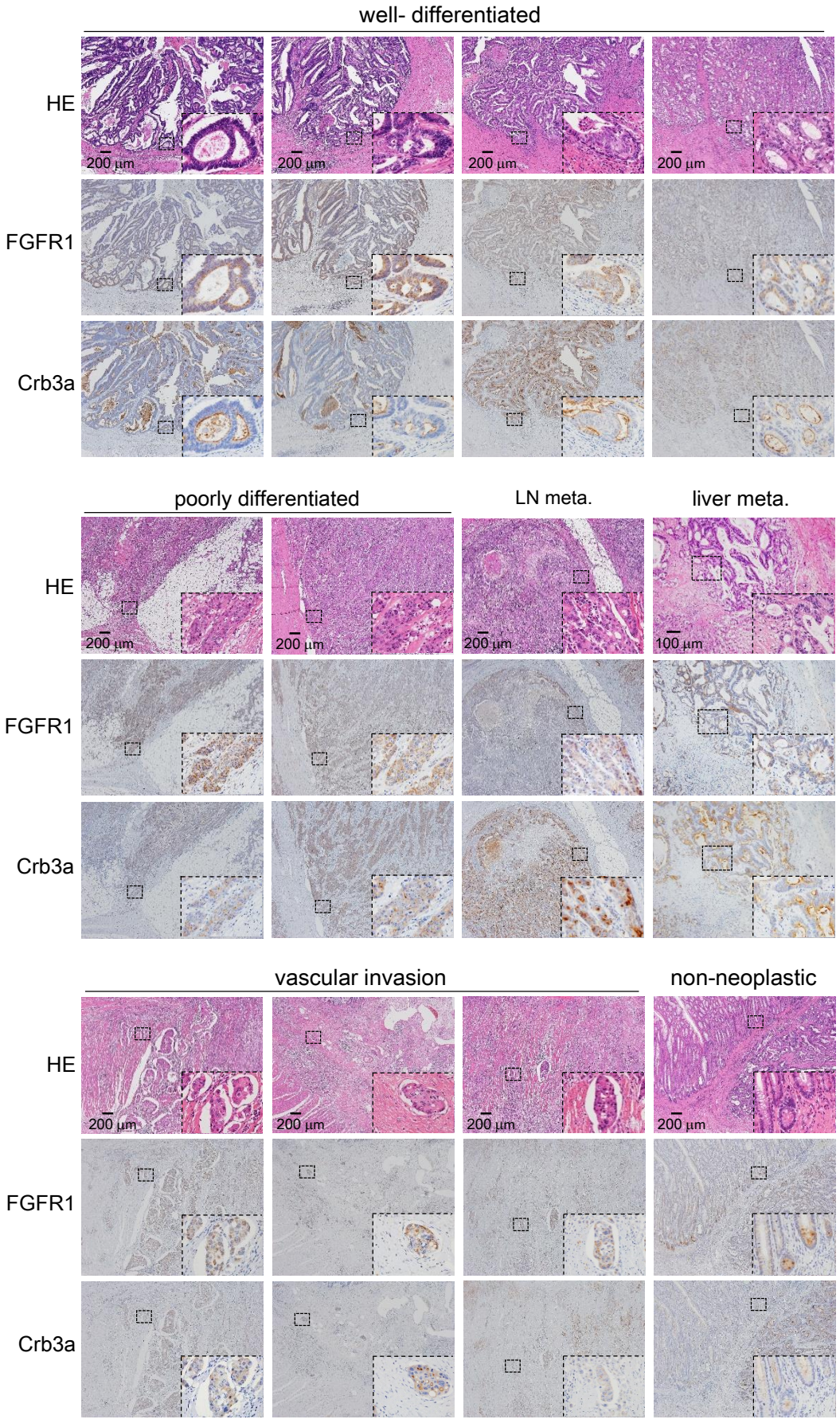

Supporting Information Figure 7 Iioka et al.

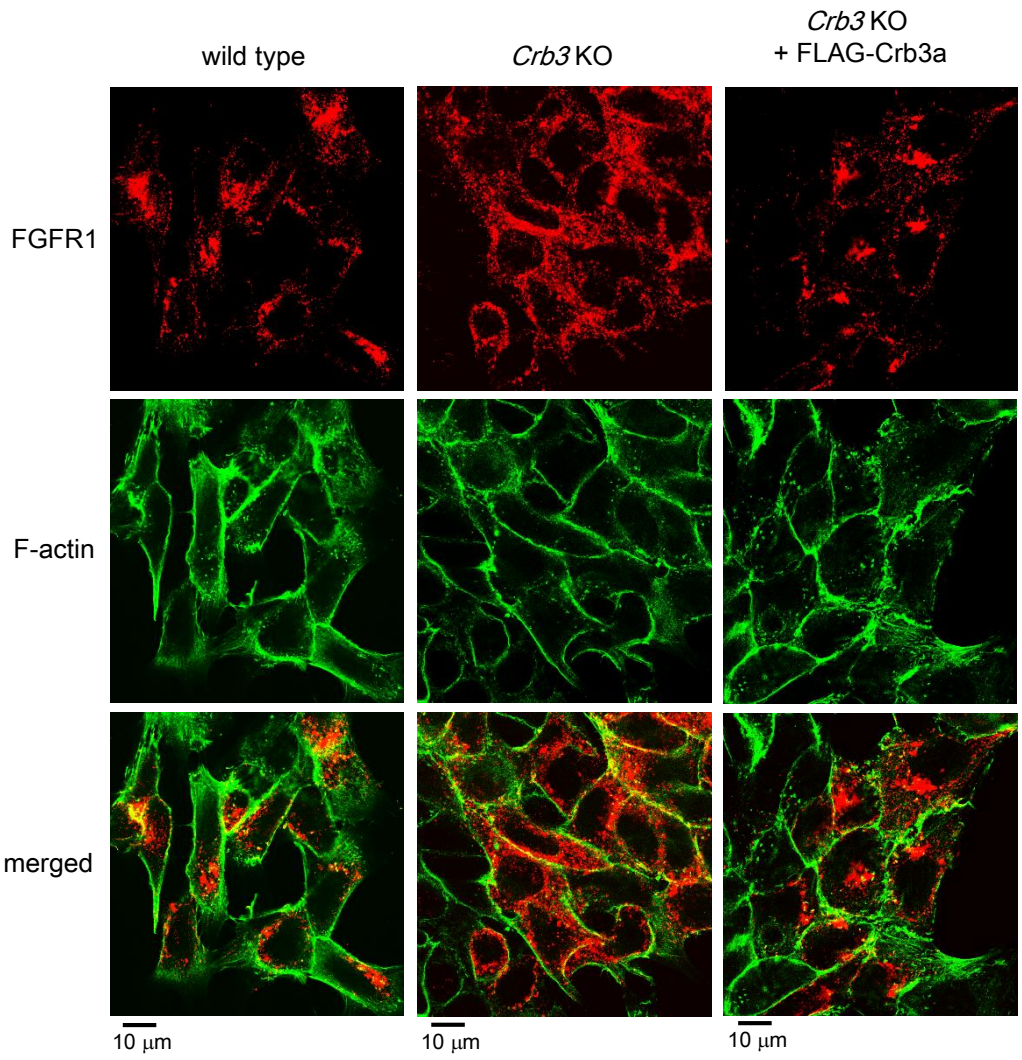

Supporting Information Figure 8 Iioka et al.

primers for transient expression vectors	sequence (5' to 3')	application	digestion	plasmid
Crb3a.Fwd.EcoRI	CGCGAATTCACCATGGCGAACCCCG GGCTG	N-terminal Crb3a amplification	EcoRI, NheI	pcDNA3-FLAG-Crb3a, pcDNA3-FLAG-Crb3b, pcDNA3-FLAG-Crb3ΔCter
extag.R-Nhe	GCCGCTAGCCAAAACAGTGCTATTCT CATTTGC			
extag.F-Mlu	GCCACGCGTCCTTCATCCACCAGCT CCA	C-terminal Crb3a, Crb3b amplification	MluI, XhoI	
Crb3a.Rvs.XhoI.stp	GCGCTCGAGTCAGATGAGCCGCTCT TCCGG			
Crb3b.Rvs.XhoI.stp	GCGCTCGAGCTAGATGGGCAGGCA GCCCTG			
Crb3Δ1.Rvs.Xho.stp	CGCCTCGAGTTACTGCTCCTCGCTA CTGGG			
FLAG.Nhe.F	GCCGCTAGCGACTACAAGGACGACG ACGACAAGGGCGGCGACTACAAGGA CGACGACGACAAG	FLAG-tag fragment	NheI, MluI	pcDNA3-FLAG-Crb3a, pcDNA3-FLAG-Crb3b, pcDNA3-FLAG-Crb3ΔCter
FLAG.Mlu.R	GCCACGCGTCTTGTCGTCGTCGTCC TTGTAGTCGCC			
FGFR1.Fw.MfeI	GCGCAATTGGGGATGTGGAGCTGGA AGTGCCTCCT	FGFR1 or FGFR1Δcyto amplification	MfeI, Xho	pcDNA3-FGFR1-cHIS, pcDNA3-FGFR1Δcyto-cHIS
FGFR1.Rv.XhoI	GCGCTCGAGGCGGCGTTTGAGTCCG CCATTGGCAA			
FGFR1-dCyto.Rv.Xho	GCGCTCGAGACTCTTCTTGGTACCA CTCTTC			
FGFR2.Fw.MfeI	GCGCAATTGACCATGGTCAGCTGGG GTCGTTTCAT	FGFR2 amplification	MfeI, Xho	pcDNA3-FGFR2-cHIS
FGFR2.Rv.XhoI	GCGCTCGAGTCTTGGGTCAGGATAA CAAGGTGAATAC			
FGFR4.Fw.EcoRI	CGCGAATTCGAGATGCGGCTGCTGC TGGCCCTGTTG	FGFR4 or FGFR4Δcyto amplification	EcoRI, Xho	pcDNA3-FGFR4-cHIS pcDNA3-FGFR4Δcyto-cHIS
FGFR4.Rv.XhoI	GCGCTCGAGTGTCTGCACCCCAGAC CCGAAGGGGAA			
FGFR4-dCyto.Rv.Xho	GCGCTCGAGCCGGCCGTGGAGCGC CTGCCC			
cHis-XhoSal.F	TCGAGGGCCACCACCATCACCATCA CTAAG	HIS-tag addition to FGFR plasmids	XhoI, SalI	FGFR plasmids
cHis-XhoSal.Rv	TCGACTTAGTGATGGTGATGGTGGT GGCCC			

primers for lentiviral plasmid construction	sequence (5' to 3')	application	insertion	plasmid
pcDNA3.to.pWPI.Fw.inf	CTAGCCTCGAGGTTTCGACTCACTAT AGGGAGACCC	Infusion cloning	PmeI site in pWPI vector	pWPI-FLAG-Crb3a pWPI-FGFR1-cHIS pWPI-FGFR1Δcyto-cHIS
pcDNA3.to.pWPI.Rv.inf	TGCAGCCCGTAGTTTTGACACTATAG AATAGGGCCC			

primers for RT-PCR	sequence (5' to 3')
FGFR1.RT.Fw	ATCCATGAACTCTGGGGTTCTTC
FGFR1.RT.Rv	AGGCATACTCCACGATGACATAC
FGFR4.RT.Fw	GTTTCCCCTATGTGCAAGTCCTA
FGFR4.RT.Rv	TGGGTCGAGAGGTAGATCTAGAC
Crb3.RT.common.Fw	GAAGCCATCACTGCTATCATCGT
Crb3.RT.common.Rv	GCGCTCGAGCTAGATGGGCAGGCA GCCCTG

siRNAs	target sequence (5' to 3')	product #	manufacturer
siCrb3-1	CAGGGAAGAAGGUACUUCA	s40936	Ambion
siCrb3-2	AGUGCUUAAUAGCAGGGAA	s195567	Ambion
siFGFR1-1	GCAUUGUGGAGAAUGAGUA	s5165	Ambion
siFGFR1-2 (mixture of 4 siRNAs)	GCCACACUCUGCACCGCUA	L-003131-00-0005	Dharmacon
	CCACAGAAUUGGAGGCUAC		
	CAAAUGCCCUUCCAGUGGG		
	GAAAUUGCAUGCAGUGCCG		
siFGFR4-1	CAUUGACUACUAUAAGAAA	s5176	Ambion
siFGFR4-2	CCACCACAUUGACUACUAU	s5177	Ambion

Supporting Information Table1 Iioka et al.

Supporting Information legends

Supporting Information Figure 1. Crb3 expression in cancer cell lines. (*a*) Specificity of anti-Crb3a antibody was evaluated by the absorption test. Wild type (wt) or *Crb3*-KO DLD-1 cell lysate was analyzed by immunoblot using anti-Crb3a antibody with or without Crb3a peptide. Normal mice IgG is employed as a negative control. (*b*) The empty vector, FLAG-Crb3a or FLAG-Crb3b expression plasmids were transfected into HEK293T cells, and demonstrated immunoblot using anti-Crb3a antibody. (*c*) Representative images of immunohistochemistry and color-deconvolution for semi-quantification of Crb3a staining. Intensity of the staining of normal colon crypts or tumor tissues were measured by setting up regions of interest (red) using the ImageJ software. (*d*) Crb3a staining intensity on immunohistochemistry was compared among normal colon crypts, tubular adenocarcinomas and liver metastases form same patients. Daggers represents statistical significance ($p < 0.01$). (*e*) Crb3a staining intensity on immunohistochemistry was compared between the normal colon crypts and poorly-differentiated adenocarcinomas in same slides. The dagger represents statistical significance ($p < 0.01$).

Supporting Information Figure 2. Crb3 regulates colon adenocarcinoma cell mobility. (*a*) Subcellular localization of endogenously expressed Crb3a protein in colon cancer cell lines was analyzed by immunofluorescent. (*b*) Gene mutation of *Crb3*-KO DLD-1 cells was validated by Sanger sequencing. Genomic DNA sequence around *Crb3* gRNA target site was analyzed. (*c*) Anchorage-independent proliferation of wt and *Crb3*-KO DLD-1 cells were examined by colony-forming assay. (*d*) Anchorage-independent proliferation

of wt and *Crb3*-KO WiDr cells were examined by colony-forming assay. (*e*) Invasiveness of wild type and *Crb3*-KO DLD-1 cells were assayed using matrigel coated transwell chambers. Right panels indicate representative image of invaded cells stained with 20% methanol / 0.1% crystal violet.

Supporting Information Figure 3. *Crb3* deficient DLD-1 displayed significant reduction in metastatic potential. (*a*) *Crb3* deficiency was examined in DLD-1 human colon cancer xenograft in NOD/SCID mice. Right panels indicate intraabdominal tumors. *b*) Quantification of total intraperitoneal tumor weight of wt or *Crb3*-KO DLD-1 injected mice. The data indicate mean ± SD of total tumor weight in single mice (n=7), and the dagger represents statistical significance ($p < 0.01$). Statistical significance was tested using unpaired two-tailed student's t-test. (*c*) Immunohistochemistry of wt and *Crb3*-KO DLD-1 xenograft tumor formed in NOD/SCID mice using anti-Crb3a antibody. Bottom panels indicate HE staining on the same visual field in serial sections.

Supporting Information Figure 4. Tumor progression in mice bearing WiDr xenograft was not altered by deficiency of *Crb3*. (*a*) *Crb3* deficiency was examined in WiDr human colon cancer xenograft in NOD/SCID mice. Right panels indicate intraabdominal tumors. (*b*) Statistically significant difference was not observed in tumor formation between wt and *Crb3*-KO WiDr cell injected mice. (*c*) Immunohistochemistry of wt and *Crb3*-KO WiDr xenograft tumor formed in NOD/SCID mice using anti-Crb3a antibody. Bottom panels indicate HE staining on the same visual field in serial sections.

Supporting Information Figure 5. Crb3a regulates FGFR1 signaling *in vitro*. (*a*) The

interaction between FLAG-Crb3a and HIS-tagged FGFR1, FGFR2 or FGFR4 were examined by HIS-pull down assay. (*b*) The interaction between Crb3a and Full-length FGFR4 or FGFR4Δcyto were examined by HIS-pull down assay. (*c*-*e*) wt and *Crb*3-KO DLD-1 cells stably expressing FGFR4-HIS were compared with control cells (empty) by immunoblot (*c*), MTT assay (*d*) or transwell chamber assay (*e*). Daggers represent statistical significance ($p < 0.01$). (*f* and *g*) wt or *Crb*3-KO WiDr cells stably expressing FGFR1-HIS were compared with control cells (empty) by immunoblot (*f*) or MTT assay (*g*). (*h*) DLD-1 or WiDr stably expressing HIS-tagged FGFRs were analyzed by dual-color immunofluorescence using anti-FGFR1 or anti-FGFR4 and anti-Crb3a. (*i*) *Crb3*-KO DLD-1 cells treated with control siRNA or siFGFR1were compared by transwell chamber assay. (*j*) ERK phosphorylation by recombinant FGF1 treatment was diminished in siFGFR1 treated DLD-1 cells. (*k*) Ligand stimulated ERK phosphorylation was not affected in siFGFR4 treated WiDr cells.

Supporting Information Figure 6. (*a*) *Crb*3-KO DLD-1 cells stably expressing FLAG-Crb3a were compared with control cells by immunoblot using antibodies against phosphor-FGFR1 (p-FGFR1), FGFR1, FLAG-tag or tubulin. (*b*) Conventional RT-PCR was performed using cDNA library from DLD-1, WiDr and normal human dermal fibroblast (NHDF). *Crb3a* and *Crb3b* transcripts were detected concurrently using common primes. (*c*) Domain structures and C-terminal amino acid sequences of Crb3 constructions. SP and TM indicate signal peptides and transmembrane domains respectively. (*d*) Pull-down assays using FGFR1-HIS and FLAG-Crb3b or FLAG-Crb3 Δ Cter constructs in HEK293T cells. (*e*) *Crb*3-KO DLD-1 cells stably expressing FLAG-Crb3a or FLAG-Crb3 Δ Cter were compared with control cells by immunoblot using

antibodies against phosphor-FGFR1 (p-FGFR1), FGFR1, FLAG-tag or tubulin. (*f*) *Crb*3-KO DLD-1 cells stably expressing FLAG-Crb3a or FLAG-Crb3 ΔCter were compared with control cells by transwell chamber assay. (*g*) The expression epithelial-mesenchymal transition related proteins were not altered by the deficiency of *Crb3* in DLD-1 cells.

Supporting Information Figure 7. Crb3 and FGFR1 were coexpressed in patient-derived colon adenocarcinoma tissues. Immunohistochemistry was performed using anti-FGFR1 or anti-Crb3a on tissues including non-neoplastic colon crypts, primary lesion and metastatic foci. Panels indicate the same visual field in serial sections.

Supporting Information Figure 8. Deficiency of Crb3 altered FGFR1 localization in DLD-1 cells**.** Wild type DLD-1, *Crb3*-KO and revertant cells stably expressing FGFR1-HIS were analyzed by immunofluorescent. FGFR1 was detected using anti-HIS antibody (red). Counterstaining of F-actin was done with Alexa488-conjugated phalloidin (green).

Supporting information Table1. The list of primers and siRNAs used in this study.